Heliyon 8 (2022) e09443

Contents lists available at ScienceDirect

Heliyon

journal homepage: www.cell.com/heliyon

Research article

# Moisture desorption behavior and thermodynamic properties of pulp and seed of jambolan (*Syzygium cumini*)

Adriano Lucena de Araújo [a], Rosinelson da Silva Pena [a,b,*]

[a] Graduated Program in Food Science and Technology, Institute of Technology, Federal University of Pará (UFPA), 66075-110, Belém, Pará, Brazil
[b] Faculty of Food Engineering, Institute of Technology, Federal University of Pará (UFPA), 66075-110, Belém, Pará, Brazil

ARTICLE INFO

*Keywords:*
*Myrtaceae*
Equilibrium moisture
Mathematical modeling
Thermodynamics

ABSTRACT

The study objectives were to establish isotherms and thermodynamic properties for the moisture desorption process of jambolan pulp (JP) and jambolan seed (JS), harvested in the city of Belém (Brazil). These characteristics can contribute for the proper selection of the operating drying conditions. Thus, the following essays were made for both JP and JS. Firstly, proximate composition was performed, followed by moisture desorption essays at 25, 35, 45 and 55 °C. In addition, six mathematical models were fitted to the experimental data to simulate the desorption behavior; and based on the chosen models, the thermodynamic properties were calculated. The results have shown that JP isotherms followed the typical behavior of products rich soluble solids, and JS isotherms were more influenced by protein components. The influence of temperature was evidenced throughout the entire range of water activity ($a_w$) studied. The GAB and Oswin models represented the best fitted equations for the JP and JS, respectively. In general, the energies involved in the desorption process of jambolan showed a greater dependence of JP with the equilibrium moisture content (EMC), in comparison with JS. Still, there was an increasing tendency of the thermodynamic properties with EMC decreasing. Besides of being non-spontaneous processes, desorption phenomena of JP and JS were enthalpy-driven mechanisms.

## 1. Introduction

*Syzygium cumini* is a tropical fruit from the *Myrtaceae* family, popularly known as jambolan, jamun, black plum or java plum. This berry presents an ovoid form, a skin varying from purple-red to black color in the ripe stages, and a total length of 2–3 cm. It also presents an astringent taste in a freshly pink/white pulp (Faria et al., 2011). All parts of the fruit, besides their nutritional constituents, contain many phytochemicals, and thus, they are widely used for medicinal purposes (Paul and Das, 2019). Some of the fruit's constituents have been attributed to the presence of anthocyanins, flavonoids, and terpenes (Aqil et al., 2014).

Jambolan, however, presents a short seasonal availability and a high perishable nature, which enhances the use of preservative techniques for lowering the moisture content of these fruits and make them available throughout the year (Paul and Das, 2019). There are still few works regarding the use of new processes that can improve the shelf life of jambolan; in this sense, drying can be used as the preservative process and the dried pulp could be used as food ingredient in the preparation of new products. Moreover, due to the large application in the traditional medicine, jambolan pulp and seed have a great potential for commercialization in the dried state, facilitating the transportation and storage stages as well.

In order to optimize the drying processes and guarantee stability of the dried products during storage, the knowledge of the product's moisture sorption isotherms is necessary, which expresses the graphical relationship between the food's equilibrium moisture content (EMC) and its correspondence water activity ($a_w$), over a range of $a_w$ values and at constant temperature (Damodaran, 2017).

Brunauer et al. (1938) classified sorption isotherms by their shape and processes. Type II is one of the most frequent isotherms in foods, and may be classified into three zones. In general, a hypothetical food system of the first zone is associated with small quantities of water and its molecules are tightly bound to polar sites. In zone II, the water is less bound, occurring as multilayer, right after the monolayer. At this region, chemical and biochemical reactions take place. In zone III, water fills the macro capillaries, exhibiting almost the full properties of bulk water, as microbial growth becomes the major deteriorative reaction (Aguilera and Stanley, 1999).

Furthermore, foodstuffs rich in soluble compounds, such as sugars, usually behave as type III, according to the classification mentioned in

* Corresponding author.
*E-mail address:* rspena@ufpa.br (R.S. Pena).

https://doi.org/10.1016/j.heliyon.2022.e09443
Received 29 October 2021; Received in revised form 3 January 2022; Accepted 11 May 2022

the previous paragraph. Falade and Aworh (2004) theorizes that, at low $a_w$ values, it can occur a local dissolution of sugar alcohols, a swelling of proteins and an arising of new active sites. In the intermediate $a_w$ range, sorption appear at the less active sites, while at higher $a_w$, dissolution of sugars gradually takes place and results in the complete exudation of sugars in solution.

In the case of fresh fruits and seeds, desorption isotherms are essential tools in the drying stages, working for the proper selection of operating conditions in regard to drying, packaging, and storage requirements for a desired shelf life. For this, thermodynamic properties of moisture sorption have been appointed as one of the approaches used to understand the water properties in the food matrix, and calculate the energy demands of heat and mass transfer in the food drying (Khiari et al., 2020).

The study of these thermodynamic properties is of great importance for the projection and dimensioning of equipment in several preservation processes. Such properties include enthalpy, entropy, Gibbs free energy and enthalpy-entropy compensation theory; featuring essential roles in describing the reactions and phenomena that occur at the intermolecular level in food materials (Sormoli and Langrish, 2015).

No literature was found for sorption isotherms of jambolan seeds, only studies involving other seeds (Prette et al., 2013; Aslan-tontul, 2020). In contrast, some current works have analyzed the moisture sorption characteristics of fresh jambolan pulp (Biswall et al., 2017), freeze-dried jambolan (Santana et al., 2014), and microwave-convective hot air dried jambolan (Paul and Das, 2019). The latter work focused on evaluating the hygroscopic behavior from a mixture composed by the pulp and seed powders of jambolan. The present study, however, evaluated the hygroscopic behavior for both pulp and seed of jambolan, separately. Furthermore, no studies have contemplated the thermodynamic properties of fresh jambolan pulp and seed, separately, in order to understand better the energy requirements for their drying processes.

Thus, this study aimed: (I) to determine the desorption isotherms of jambolan pulp and seed in a relative humidity (RH) range of 90–10%, at 25, 35, 45 and 55 °C; (II) to define the most suitable model fitted to the desorption isotherms for jambolan pulp and seed; and (III) to estimate the thermodynamic properties of moisture desorption for jambolan pulp and seed.

## 2. Material and methods

### 2.1. Raw material

Jambolan (*Syzygium cumini*) fruits were harvested during the rainy season, in the period of December 2020 to January 2021, from trees located at the Federal University of Para – UFPA (latitude 1°28' S, longitude 48°29′ W), in the city of Belém (Brazil). It is worth mentioning that this study refers only to the jambolans grown in the city of Belém. The climate of this region is tropical monsoon, with annual air temperature between 22 °C to 31.5 °C, and daily precipitations around 25 mm, at average (INMET, 1992). In Brazil, jambolan flowering goes from September to November, and the full ripening goes from December to February (Sabino et al., 2018).

Right after harvesting, ripe fruits were transported in polystyrene isothermal boxes to the Laboratory of fruits at UFPA. Posterior to discard of the injured jambolans, the fruits were rinsed in running water, and sanitized by immersion in hypochlorite solution at 20 mg/L of active chlorine for 15 min, followed by rinsing and drying with an absorbent paper, as described by Araújo and Pena (2021). Then, jambolan pulp (JP) was separated from the jambolan seed (JS), with a stainless steel laboratory spatula, in order to proceed with the next analyzes.

### 2.2. Proximate composition

JP and JS were submitted to the following analyzes: moisture content (n. 934.06), ashes (n. 940.26), total proteins (with a nitrogen-to-protein conversion factor of 6.25) (n. 920.152) and total lipids (n. 945.38F). These procedures were performed according to the Association of Official Analytical Chemists (AOAC, 2010) methodology. In addition, carbohydrates were calculated by the difference between 100 and the sum from the percentage of moisture, total proteins, total lipids and ashes (FAO, 2003). Water activity ($a_w$) was determined by direct reading in the Vapor Sorption Analyzer (VSA) (Aqualab VSA, Decagon, USA). The experiments were obtained in triplicates, expressed as mean ± standard deviation.

### 2.3. Moisture desorption data acquisition

The moisture desorption data were acquired by the Vapor Sorption Analyzer (VSA). The following procedure was adopted for both JP and JS: approximately 2000 mg of sample were weighed in an analytical balance (M214AIH, BEL, Brazil), and ground with the aid of a mortar and a pestle. Before initiating the desorption test, the ground sample was placed inside the glass desiccator, with silica gel at the base, to decrease the $a_w$ level of the sample. This step was interrupted when the sample reached around 0.9 $a_w$. Subsequently, around 1600–1800 mg of the sample were weighed in the stainless steel capsule of the VSA, using the equipment's own micro analytical balance. The equipment was programmed to obtain desorption data in the range of 0.9 to 0.1 $a_w$, through the Dynamic Vapor Sorption (DVS) method. The condition of equilibrium was arranged for a change in mass per change in time (trigger % dm/dt value) below 0.1 for two consecutive measures. The device was arranged to obtain the equilibrium data in 0.1 $a_w$ intervals. After completing the analysis, the sample's dry mass was determined in the drying oven at 105 °C. Desorption isotherms were obtained at 25, 35, 45, and 55 °C, for both JP and JS.

### 2.4. Desorption isotherms modeling

The monolayer moisture content ($m_o$) for each temperature analyzed (25, 35, 45 and 55 °C) was determined by linear regression using the linearized form of the BET equation (Eq. (1)) (Brunauer et al., 1938). This model was used to calculate the desorption $m_o$ of JP and JS, in the $a_w$ range from 0.4 to 0.1.

$$\frac{a_w}{(1-a_w)m} = \frac{1}{m_o C} + \frac{(C-1)}{m_o C} a_w \tag{1}$$

where: m = equilibrium moisture content (g $H_2O$/100 g dry basis); $a_w$ = water activity (dimensionless); $m_o$ = monolayer moisture content (g $H_2O$/100 g db); C = constant related to the sorption heat.

The following mathematical models (Eqs. (2), (3), (4), (5), (6), and (7)) (Chirife and Iglesias, 1978; Chowdury and Das, 2010; Maroulis et al., 1988) were tested to fit the desorption data of JP and JS at different temperatures:

$$\text{GAB:}\quad m = \frac{m_o.c.k.a_w}{[(1-k.a_w).(1+(c-1).k.a_w]} \tag{2}$$

$$\text{Halsey:}\quad m = \left[\frac{-a}{\ln a_w}\right]^{\frac{1}{b}} \tag{3}$$

$$\text{Oswin:}\quad m = a.\left[\frac{a_w}{1-a_w}\right]^{b} \tag{4}$$

$$\text{Henderson:}\quad m = \left[\frac{-\ln(1-a_w)}{1-a_w}\right]^{\frac{1}{b}} \tag{5}$$

$$\text{Smith:}\quad m = b + a.\ln(1-a_w) \tag{6}$$

$$\text{Peleg:}\quad m = k_1.a_w^{n_1} + k_2.a_w^{n_2} \tag{7}$$

where: m = equilibrium moisture content (g $H_2O$/100 g db); $a_w$ = water activity (dimensionless); $m_o$ = monolayer moisture content (g $H_2O$/100 g db); a, b, c, $k_1$, $k_2$, $n_1$, $n_2$ = model constants.

### 2.5. Thermodynamic properties calculation

The net isosteric heat of desorption ($q_{st}$) or differential enthalpy of desorption (ΔH) was determined by Eq. (8), from the angular coefficient of the line obtained by the ln($a_w$) versus 1/T correlation, for different levels of moisture content. In turn, the isosteric heat of desorption ($Q_{st}$) was calculated by adding to $q_{st}$ the latent heat of vaporization of pure water ($\lambda_{vap}$) (Eq. (9)), at the mean temperature of the desorption processes (40 °C) (Rizvi, 2014).

$$q_{st} = -R\left[\frac{d(\ln a_w)}{d(1/T)}\right] \tag{8}$$

$$Q_{st} = q_{st} + \lambda_{vap} \tag{9}$$

where: R = gas constant (0.4619 kJ/kg.K); $a_w$ = water activity (dimensionless); T = absolute temperature (K); $\lambda_{vap}$ = latent heat of vaporization of pure water at the average of the temperatures considered in this study (2,405.1 kJ/kg at 40 °C).

The change in differential entropy (ΔS) was calculated according to Eq. (10), from the linear coefficients (ΔS/R) of the slope ln($a_w$) versus 1/T correlation, for different levels of moisture content. The Gibbs free energy was calculated from Eq. (11) (Rizvi, 2014).

$$-\ln(a_w)|_m = \frac{Q_{st}}{RT} - \frac{\Delta S}{R} \tag{10}$$

$$\Delta G = -RT \ln a_w \tag{11}$$

where: ΔS = change in differential entropy (kJ/kg.K); ΔG = Gibbs free energy (kJ/kg).

Moreover, the enthalpy–entropy compensation theory is a linear relationship between ΔH and ΔS. From the ΔH *versus* ΔS graphic, the isokinetic temperature ($T_\beta$) could be determined (Eq. (12)). To validate the compensation theory, a statistical test is recommended and consists in the comparison between $T_\beta$ and the harmonic mean temperature ($T_{mh}$), obtained by the following equation (Eq. (13)) (Krug et al., 1976).

$$\Delta H = \Delta G + T_\beta.\Delta S \tag{12}$$

$$T_{hm} = \frac{n}{\sum_1^n (1/T)} \tag{13}$$

where: $T_\beta$ = the isokinetic temperature (K); $T_{hm}$ = the harmonic mean temperature (K); n is the number of isotherms.

For the $Q_{st}$ prediction, the following model was tested (Eq. (14)), for JP and JS. This equation was proposed by Mulet et al. (1999).

$$Q_{st} = d.\exp(-g.m) + \lambda_{vap} \tag{14}$$

where: $Q_{st}$ = isosteric heat of desorption (kJ/kg); m = equilibrium moisture content (g $H_2O$/100 g db); $\lambda_{vap}$ = latent heat of vaporization of pure water; d and g are model parameters.

### 2.6. Statistical analysis

The proximate composition results of JP and JS were assessed using Student's t-test, at 5% significance, for comparison of means. Nonlinear regression analysis was used to fit the mathematical models to the moisture desorption data for JP and JS. The Levenberg-Marquardt algorithm was used with a $10^{-6}$ convergence criterion. To evaluate the quality of the model fits, the coefficient of determination ($R^2$), the relative mean deviation (P) (Eq. (15)) and the distribution of residues were used.

**Table 1.** Proximate composition of jambolan pulp (JP) and jambolan seed (JS).

| Properties | Result* | |
|---|---|---|
| | JP | JS |
| Moisture (g/100 g) | $84.76^a \pm < 0.01$ | $45.64^b \pm 0.2$ |
| Ashes (g/100 g) | $0.29^b \pm 0.01$ | $0.99^a \pm < 0.01$ |
| Total lipids (g/100 g) | $0.34^a \pm 0.04$ | $0.36^a \pm 0.02$ |
| Total proteins (N × 6.25) (g/100 g) | $0.47^b \pm 0.03$ | $3.11^a \pm 0.04$ |
| Total carbohydrates (g/100 g) | $14.40^b \pm 0.03$ | $49.90^a \pm 0.23$ |
| $a_w$ at 25 °C | $0.98^a \pm < 0.01$ | $0.97^b \pm < 0.01$ |

* Mean of three replications ± standard deviation. Different letters at the same line indicate significant difference by the Student's t-test ($p \leq 0.05$).

$$P = \frac{100}{n}\sum_{i=1}^{n}\frac{|m_{exp,i} - m_{pre,i}|}{m_{exp,i}} \tag{15}$$

where: $m_{exp,i}$ and $m_{pre,i}$ = ith observed and predicted equilibrium moisture contents, respectively, and n = number of observations.

## 3. Results and discussion

### 3.1. Proximate composition of JP and JS

Table 1 presents the proximate composition for both JP and JS (in wet basis – wb), as well as the results for $a_w$ at 25 °C. These findings corroborate to the results observed by Araújo and Pena (2021), whose proximate composition, for JP, was: 84.80 ± 0.26 g/100 g moisture, 0.43 ± 0.01 g/100 g ashes, 0.56 ± 0.03 g/100 g total lipids, 0.48 ± 0.05 g/100 g total proteins, 13.90 ± 0.03 g/100 g carbohydrates; and the $a_w$ was 0.98 ± < 0.01 (25 °C). For JS, in turn, no studies have been found regarding its proximate composition.

Statistical analysis revealed significant differences ($p \leq 0.05$) between the proximate composition of JP and JS, except for total lipids. Moreover, the composition and physicochemical properties of JP and JS have evidenced their perishable nature, especially in function of the high contents of moisture and $a_w$, which may not ensure the microbial stability to JP and JS ($a_w > 0.6$) (Scott, 1957; Rahman, 2009).

### 3.2. Moisture desorption isotherms

Figure 1 shows the moisture desorption isotherms for JP and JS at 25, 35, 45 and 55 °C, highlighting the effect of temperature. The equilibrium moisture content (EMC) of JP (Figure 1A) decreased relatively fast (exponentially) at ≈ 0.9–0.5 $a_w$, in contrast with the region below 0.5 $a_w$, in which a linear decrease was observed for all temperatures studied. The desorption isotherms from JS (Figure 1B), in turn, indicated that when the $a_w$ value drops from 0.9 to 0.7, the isotherms undergo an exponential decrease. Below this $a_w$ level, a linear behavior was evidenced. Thus, under these conditions (90% ≥ RH ≥ 50% for JP, and 90% ≥ RH ≥ 70% for JS), the products will be more susceptible to moisture loss and, therefore, small changes in RH lead to great changes in EMC. According to Brunauer et al. (1938) classification, the JP isotherms (Figure 1A) presented a type III behavior, which is a characteristic of foods rich in soluble solids, while JS isotherms (Figure 1B) showed type II behavior, indicating the presence of protein components. However, JP isotherms followed the type II - more to the solution-like behavior, while JS isotherms followed the behavior of type II - more to the Langmuir-like, according to the quantitative criteria established by Yanniotis and Blahovec (2009). These results are in agreement with JP and JS composition, found in Table 1.

Regarding JP isotherm shapes, similar trends were evidenced in freeze-dried jambolan (Santana et al., 2014), microwave-convective hot

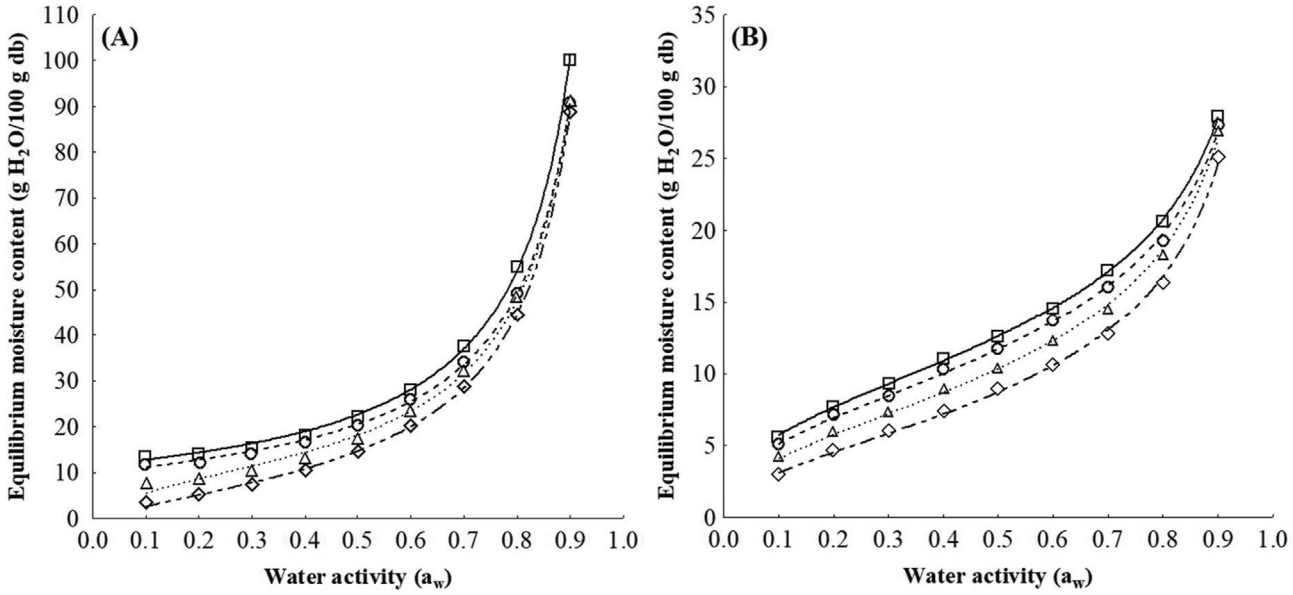


**Figure 1.** Moisture desorption isotherms of JP (A) and JS (B), at 25 °C (□), 35 °C (○), 45 °C (△), 55 °C (◇), and predicted data from the GAB (A) and Oswin (B) models, at 25 °C (——), 35 °C (- - - - -), 45 °C (·····), and 55 °C (— – – —).

air dried jambolan (Paul and Das, 2019) and fresh jambolan (Biswall et al., 2017). On the other hand, jackfruit seeds (Prette et al., 2013) and chinoa seeds (Aslan-tontul, 2020) followed a sigmoid format, as observed in JS.

At constant $a_w$, the EMC decreases as the temperature increases, which indicates that both JP (Figure 1A) and JS (Figure 1B) are less hygroscopic at high temperatures. This phenomenon is attributed to the excitation states of molecules due to temperature increasing, which increases their distance and; therefore, decreases the attractive forces between them (Hassini et al., 2015). Additionally, it can be stated that the JP will be microbiologically stable ($a_w < 0.6$) (Scott, 1957) when its moisture content is less than 28.04 g $H_2O$/100 g db, if stored at 25 °C. For JS, this stability corresponds to a moisture content value of less than 14.55 g $H_2O$/100 g db (25 °C); half of the observed value for JP. However, if the temperature is extrapolated, the limiting moisture content for JP continuously drops to 25.84, 23.26, and 20.16 g $H_2O$/100 g db, at 35, 45 and 55 °C, respectively. Moreover, the JS's limiting moisture content value will drop to 13.68, 12.30, and 10.60 g $H_2O$/100 g db, if the temperature is equivalent to 35, 45 and 55 °C, respectively.

Still, according to isotherms (Figure 1), JP is more hygroscopic than JS, at all $a_w$ and temperature range studied. The minimum EMC variation observed between JP and JS isotherms, for a same $a_w$ level, was 6.12 g $H_2O$/100 g db (25 °C), 5.03 g $H_2O$/100 g db (35 °C), 2.62 g $H_2O$/100 g db (45 °C) and 0.45 g $H_2O$/100 g db (55 °C), in the range of $a_w$ from 0.1 to 0.3. The greatest variations occurred in $a_w$ levels above 0.6, when there were observed EMC variations from 13.49 to 72.21 g $H_2O$/100 g db at 25 °C, 12.16–63.43 g $H_2O$/100 g db at 35 °C, 10.96–64.33 g $H_2O$/100 g db at 45 °C and 9.57–63.80 g $H_2O$/100 g db at 55 °C. The EMC variation increased with $a_w$ increasing, and it was higher at 25 °C.

### 3.3. Mathematical modeling

The fits of the linearized form of the BET model (Eq. (1)) to the experimental data generated desorption monolayer moisture content ($m_o$) values of 10.56 g $H_2O$/100 g db (25 °C), 9.75 g $H_2O$/100 g db (35 °C), 8.06 g $H_2O$/100 g db (45 °C) and 7.84 g $H_2O$/100 g db (55 °C), for JP ($R^2 > 0.95$). In turn, desorption $m_o$ values for JS corresponded to 7.08 g $H_2O$/100 g db (25 °C), 6.60 g $H_2O$/100 g db (35 °C), 5.86 g $H_2O$/100 g db (45 °C) and 5.08 g $H_2O$/100 g db (55 °C), with $R^2 > 0.99$. The $m_o$ values decreased with temperature increasing. This behavior is already expected, since the increase in temperature elevates the energy level of water molecules and promotes the detachment between the interaction sites of water and solute, thus decreasing the stability of water molecules bonding and resulting in the reduction of EMC at a given $a_w$ value (Palipane and Driscoll, 1993; Pahlevanzadeh and Yazdani, 2005).

The behavior observed for $m_o$ diverged from the study of Santana et al. (2014), who found values of $m_o$ in the order of 7.64 g $H_2O$/100 g db at 25 °C and 12.08 g $H_2O$/100 g db at 35 °C for the freeze-dried jambolan. The authors suggested that the unusual behavior occurred probably due to modifications in the three-dimensional rearrangement, where the polar groups became available, and the solubility increased with temperature increasing. For practical purposes, the value of $m_o$ for the desorption process indicates the moisture content limit, from which it is no longer necessary to extend the drying stage for JP and JS, to avoid unnecessary power consumption.

As previously mentioned, the suitability of the fits was assessed by means of $R^2$, P and residual plots, for the desorption isotherms of JP and JS, at different temperatures (Table 2). According to the statistical results, the equations that best fitted to the experimental data were the GAB model ($R^2 > 0.99$, P < 6.4%, random residues) for JP and the Oswin model ($R^2 > 0.99$, P < 2.3%, random residues) for JS.

Generally, models with a P value of less than 10% are considered acceptable for practical purposes (Peng et al., 2007). However, to ensure that the suitable model is able to express a given phenomenon, the residues' dispersion should be verified for the different models; since, even if the statistical parameters show good fits, the model can be ineffective if it presents a biased residue distribution (Bowman and Robinson, 1990). Thus, these models (GAB - JP, Oswin - JS) have been chosen not only by their lowest P values (at average), but also by their random distribution of residues, at all temperatures studied. It is worth mentioning that, although Peleg's equation was not chosen to represent the desorption data, it also showed good fits for both JP and JS. The Peleg model is an equation with four parameters, which justifies its good fit. However, Peleg's equation has a more difficult mathematical solution.

GAB equation has a theoretical background, and it is a refinement of the Langmuir and BET theories of physical adsorption. This model was suitable for analyzing many pulp fruits, including jackfruit pulp (Prette et al., 2013), murtilla berry (Ah-hen et al., 2014), jambolan fruits (Biswall et al., 2017), and Italia grapes (Khiari et al., 2020). Otherwise, Oswin's model has been widely fitted to foodstuffs, displaying good

**Table 2.** Mathematical modeling parameters for the desorption process of JP and JS.

| Model/Parameter | | Jambolan pulp (JP) | | | | Jambolan seed (JS) | | | |
|---|---|---|---|---|---|---|---|---|---|
| | | Temperature (°C) | | | | | | | |
| | | 25 | 35 | 45 | 55 | 25 | 35 | 45 | 55 |
| GAB | $m_o$ | 11.5 | 10.49 | 10.33 | 10.18 | 7.90 | 7.10 | 6.06 | 5.15 |
| | c | $2.2 \times 10^5$ | 170.27 | 8.22 | 2.74 | 24.20 | 25.57 | 21.76 | 14.50 |
| | k | 0.990 | 0.983 | 0.99 | 0.99 | 0.80 | 0.82 | 0.86 | 0.88 |
| | $R^2$ | 0.994 | 1.000 | 0.998 | 1.000 | 0.998 | 0.995 | 0.997 | 0.997 |
| | P | 2.62 | 2.62 | 6.32 | 3.98 | 1.66 | 2.70 | 3.02 | 3.59 |
| | Residues | R | R | R | R | B | R | R | B |
| Halsey | a | 39.03 | 34.80 | 19.43 | 11.27 | 174.27 | 115.66 | 54.58 | 27.33 |
| | b | 1.28 | 1.29 | 1.16 | 1.04 | 2.21 | 2.11 | 1.90 | 1.72 |
| | $R^2$ | 0.996 | 0.997 | 0.999 | 0.999 | 0.989 | 0.992 | 0.994 | 0.993 |
| | P | 7.46 | 6.22 | 4.19 | 10.25 | 6.08 | 5.80 | 5.69 | 7.84 |
| | Residues | B | B | R | B | B | B | B | B |
| Oswin | a | 23.14 | 20.96 | 17.75 | 14.38 | 12.63 | 11.71 | 10.36 | 8.72 |
| | b | 0.66 | 0.66 | 0.74 | 0.83 | 0.36 | 0.38 | 0.43 | 0.47 |
| | $R^2$ | 0.982 | 0.984 | 0.996 | 1.000 | 1.000 | 0.999 | 0.999 | 0.999 |
| | P | 15.20 | 14.42 | 11.01 | 6.00 | 0.69 | 1.22 | 1.88 | 2.25 |
| | Residues | B | B | B | B | R | R | R | R |
| Henderson | a | 0.06 | 0.06 | 0.10 | 0.14 | 0.01 | 0.01 | 0.02 | 0.05 |
| | b | 0.82 | 0.82 | 0.71 | 0.62 | 1.72 | 1.63 | 1.41 | 1.24 |
| | $R^2$ | 0.946 | 0.949 | 0.977 | 0.989 | 0.982 | 0.975 | 0.973 | 0.977 |
| | P | 26.77 | 26.44 | 26.27 | 27.09 | 7.08 | 8.32 | 10.66 | 11.51 |
| | Residues | B | B | B | B | B | B | B | B |
| Smith | a | 0.27 | 0.14 | -4.21 | -7.60 | 5.52 | 4.83 | 3.50 | 2.21 |
| | b | 38.08 | 34.47 | 36.55 | 36.84 | 9.71 | 9.51 | 9.73 | 9.44 |
| | $R^2$ | 0.928 | 0.932 | 0.939 | 0.937 | 0.996 | 0.994 | 0.993 | 0.991 |
| | P | 24.35 | 23.47 | 31.03 | 48.60 | 3.55 | 4.12 | 4.23 | 5.38 |
| | Residues | B | B | B | B | R | R | R | B |
| Peleg | $k_1$ | 156.39 | 26.15 | 145.32 | 36.07 | 17.55 | 24.95 | 27.52 | 14.66 |
| | $n_1$ | 7.01 | 0.43 | 7.53 | 1.27 | 0.51 | 7.91 | 7.92 | 0.72 |
| | $k_2$ | 26.33 | 142.70 | 26.68 | 162.56 | 21.66 | 17.28 | 15.72 | 28.86 |
| | $n_2$ | 0.36 | 7.42 | 0.69 | 9.89 | 6.28 | 0.56 | 0.60 | 8.87 |
| | $R^2$ | 0.997 | 0.997 | 0.998 | 0.999 | 0.999 | 0.998 | 0.999 | 0.999 |
| | P | 5.94 | 6.53 | 7.41 | 8.55 | 1.20 | 2.18 | 1.94 | 2.01 |
| | Residues | R | R | R | R | R | R | R | R |

$R^2$: coefficient of determination; P: standard error deviation; B: biased; R: random.

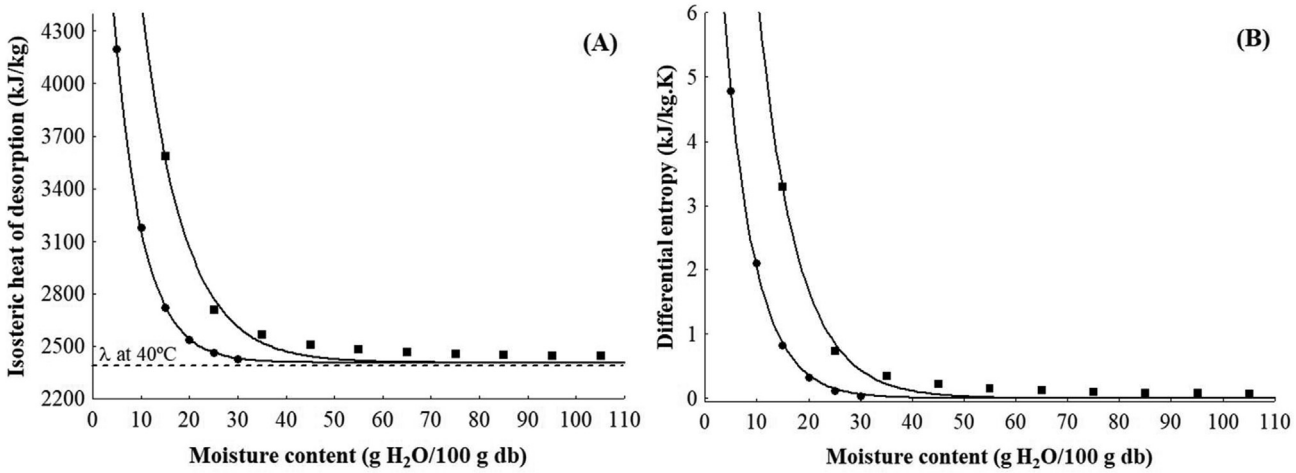


**Figure 2.** Isosteric heat of sorption (A) and differential entropy (B) for the desorption process of JP (■) and JS (●). Model fitting (——).

suitability in seeds and grains, such as jackfruit seeds (Prette et al., 2013) and prickly pear seeds (Hassini et al., 2015).

### 3.4. Thermodynamic properties

The most suitable models (GAB - JP, Oswin - JS) (Table 2) were used to calculate the thermodynamic properties of moisture desorption for JP and JS. The isosteric heat of desorption ($Q_{st}$) for JP and JS are shown in Figure 2A. The $Q_{st}$ values decreased continually with EMC increasing until 75 g $H_2O$/100 g db for JP and 30 g $H_2O$/100 g db for JS, from which the $Q_{st}$ values were close to the latent heat of vaporization of pure water at 40 °C (2,405.1 kJ/kg). Still, it can be assumed that $Q_{st}$ values were higher for JP than JS, at a same EMC. Such differences were in the order of 250.82 kJ/kg at 25 g $H_2O$/100 g db, and increased as EMC regressed; reaching variations around 870.37 kJ/kg, at 15 g $H_2O$/100 g db.

The highest $Q_{st}$ values were observed at the lowest EMC values, in which the monolayer ($m_o$) values are situated. In this region, the water molecules and the food constituents are more strongly bound, and it corresponds to the highest binding energies for water removal, since water occupies the most active available sites (Khiari et al., 2020). The increasing trend of $Q_{st}$ with EMC decreasing was also evidenced in fresh pulp and seed of jackfruit (Prette et al., 2013), in prickly pear seeds (Hassini et al., 2015) and in ryegrass seeds (Zeymer et al., 2020).

The $Q_{st}$ expresses the binding strength between the moisture-sorbent, and it is required in the designing of equipment for dehydration processes (Chowdhury and Das, 2010). In the drying industry, reaching the highest $Q_{st}$ values are undesirable in most operations as it increases the cost within the processes (Aslan-tontul, 2020).

The variation of $Q_{st}$ with EMC was fitted by the previous equation (Eq. (14)), and resulted in the equations below (Eq. (16) for JP and Eq. (17) for JS), with a confidence level of 95% ($p \leq 0.05$). In agreement with the good fits appointed by the modeling (lines) in Figure 2A, other authors observed good fits for the cassava flour data (Araújo and Pena, 2020).

$$Q_{st} = 6{,}668.2 \exp(-0.116m) + 2{,}405.1 \ (R^2 = 0.975) \quad (16)$$

$$Q_{st} = 4{,}231.1 \exp(-0.172m) + 2{,}405.1 \ (R^2 = 0.999) \quad (17)$$

Differential entropy (ΔS) for desorption process of JP and JS increases with EMC decreasing (Figure 2B). Once again, the ΔS data displayed a strong dependence on EMC. It ranged from 0.08 to 3.30 kJ/kg.K for JP and from 0.04 to 4.78 kJ/kg.K for JS. These results are in agreement with the expected for ΔS, which is a measure of the ordering change, and presents lower results when the molecular movement is more restricted, that is, when the product has higher EMC. Besides, at higher $a_w$, sites are covered with water molecules, implying in less mobility for the water molecules (Eim et al., 2011); also, ΔS of a material is proportional to the number of available sorption sites at a specific energy level (Nascimento et al., 2019), and as desorption progresses, more sites are exposed and become available. Similar results were found by Zeymer et al. (2018), in the desorption process of rice, which ΔS values varied from 0.22 to 4.64 kJ/kg.K, for an EMC variation from 21.5 to 2.6 g $H_2O$/100 g db.

At the same EMC, ΔS values were higher for JP than JS (Figure 2B). These differences were equal to 0.63 kJ/kg.K (at 25 g $H_2O$/100 g db), and increased to 2.48 kJ/kg.K (at 15 g $H_2O$/100 g db). According to the study, the variation of desorption ΔS with EMC was best fitted by the exponential model, which can be visualized in Eq. (18) for JP and Eq. (19) for JS, with a confidence level of 95% ($p \leq 0.05$). These models displayed good suitability to the ΔS data, with a slightly better adjustment for JS over JP (Figure 2B). Hassini et al. (2015) also proposed an exponential model to represent the desorption ΔS as function of EMC in prickly pear seeds.

$$\Delta S = 24.52 \exp(-0.13m) \ (R^2 = 0.986) \quad (18)$$

$$\Delta S = 11.34 \exp(-0.17m) \ (R^2 = 0.999) \quad (19)$$

From a thermodynamic point of view, Gibbs free energy (ΔG) may be used as indicative of the water and sorbent affinity, and further provide a criterion whether water sorption is a spontaneous or non-spontaneous process, depending on the sign (negative or positive) of the ΔG values (Alpizar-reyes et al., 2017). The values of ΔG for JP (Figure 3A) and JS (Figure 3B) suggest that the moisture desorption processes for both products are non-spontaneous (positive ΔG). This behavior is already expected for desorption processes, since it requires the addition of energy to occur (endergonic reaction) (Oulahna et al., 2012). Non-spontaneous desorption processes were also found in rice (Zeymer et al., 2018) and in crambe fruits (Oliveira et al., 2017).

In general, it was observed a decrease in the ΔG values as temperature increases (Figure 3), for a same EMC value, which indicate that the desorption processes of JP and JS are less viable at higher temperatures. This behavior was more evident for JP than JS, since JP is more hygroscopic (Figure 1). Also, the results showed an increasing of ΔG while EMC decreases, and the effect of temperature was more expressive in the regions below 35 g $H_2O$/100 g db for JP (Figure 3A) and 15 $H_2O$/100 g db for JS (Figure 3B). This increasing of ΔG while EMC decreased also occurred in chinoa grains, in the range of 15–35 °C (Aslan-tontul, 2020).

Furthermore, the variation of desorption ΔG followed a power model for JP and an exponential model for JS, at 95% confidence level ($p \leq 0.05$). The lines presented in Figure 3 represent the fits of the referred

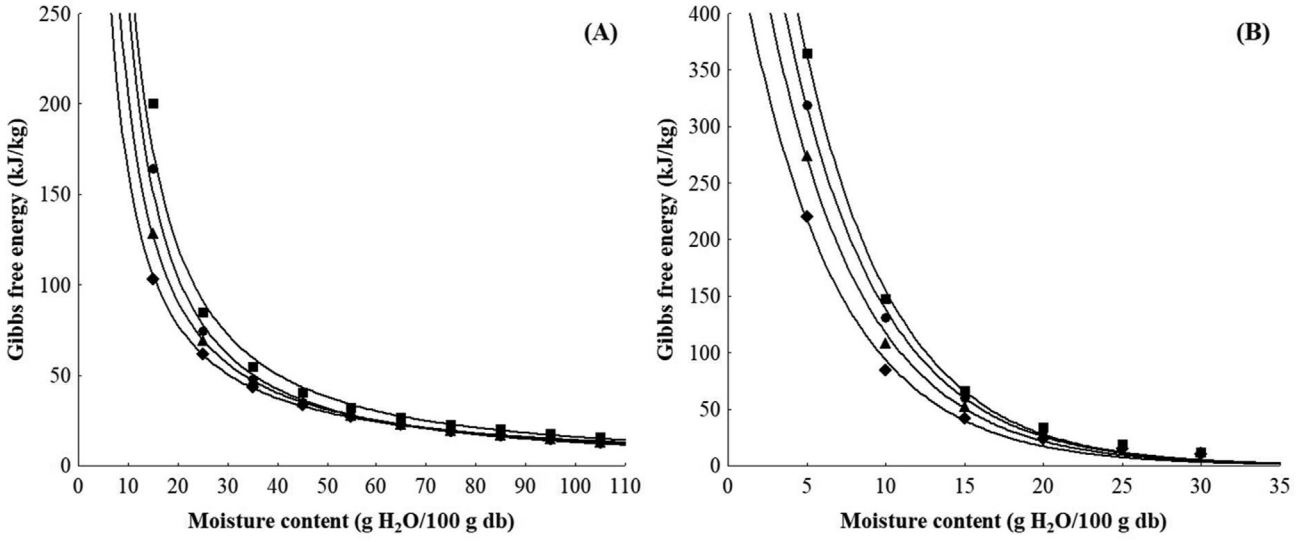


**Figure 3.** Gibbs free energy for the desorption process of JP (A) and JS (B), at 25 °C (■), 35 °C (●), 45 °C (▲), and 55 °C (◆). Model fitting (——).

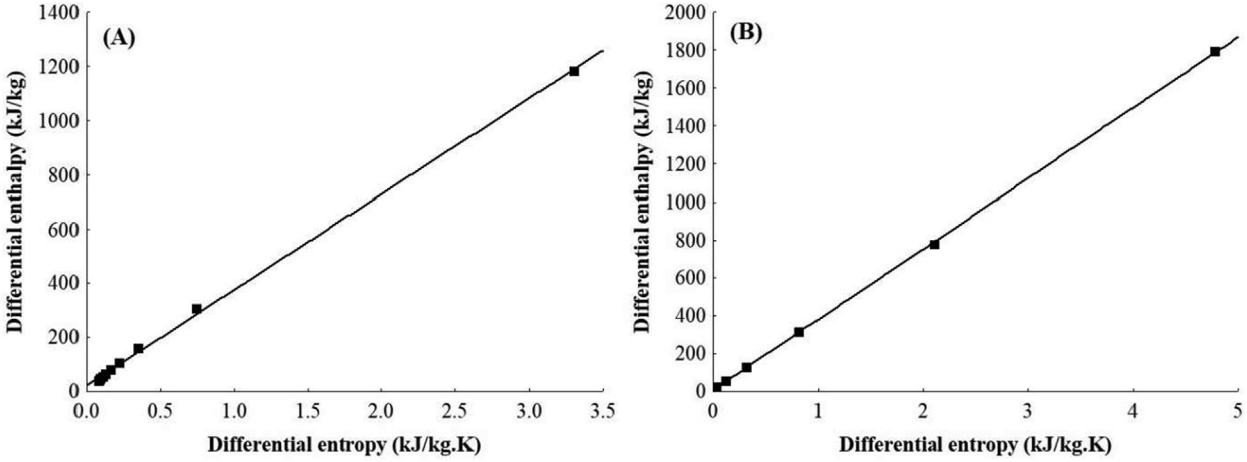


**Figure 4.** Correlation between differential enthalpy and differential entropy for the desorption process of JP (A) and JS (B). Model fitting (——).

models to the ΔG data. These good adjustments ($R^2 > 0.99$) generated the models present in Eqs. (20), (21), (22), and (23), for JP; and Eqs. (24), (25), (26), and (27), for JS.

$$\Delta G = 5{,}270.7 m^{-1.26} \ (25^{o}C) \ (R^2 = 0.992) \quad (20)$$

$$\Delta G = 5{,}058.5 m^{-1.30} \ (35^{o}C) \ (R^2 = 0.998) \quad (21)$$

$$\Delta G = 2{,}988.9 m^{-1.17} \ (45^{o}C) \ (R^2 = 1) \quad (22)$$

$$\Delta G = 1{,}839.2 m^{-1.06} \ (55^{o}C) \ (R^2 = 1) \quad (23)$$

$$\Delta G = 850.70 \exp(-0.17m) \ (25^{o}C) \ (R^2 = 0.998) \quad (24)$$

$$\Delta G = 729.19 \exp(-0.17m) \ (35^{o}C) \ (R^2 = 0.998) \quad (25)$$

$$\Delta G = 627.40 \exp(-0.17m) \ (45^{o}C) \ (R^2 = 0.995) \quad (26)$$

$$\Delta G = 505.81 \exp(-0.17m) \ (55^{o}C) \ (R^2 = 0.993) \quad (27)$$

The enthalpy-entropy compensation theory was assessed to verify the relationship between physical and chemical phenomena that might occur in the moisture desorption process of JP and JS (Figure 4). This theory states that, for minimizing changes in the free energy of these phenomena, the compensation arises with a change in the ΔH or ΔS values, through the interaction nature between solvent and solute. Thus, the ΔH and ΔS relationship follows a linear behavior, for a specific reaction (Hercigonja and Rakic, 2015).

The isokinetic temperature ($T_\beta$) was 353.5 K for JP ($\Delta H = 21.3 + 353.5\Delta S$; $R^2 = 0.999$) (Figure 4A), and 371.9 K for JS ($\Delta H = 7.41 + 371.9\Delta S$; $R^2 = 0.999$) (Figure 4B). The harmonic mean temperature ($T_{hm}$) (calculated by Eq. (13)) for both JP and JS was found to be $T_{hm} = 312.8$ K. Then, it was observed that $T_\beta \neq T_{hm}$, and this difference corroborates to the enthalpy–entropy compensation theory. The results showed that $T_\beta > T_{hm}$, and it can be assumed that the desorption processes of both JP and JS are, therefore, enthalpy-driven mechanisms (Krug et al., 1976). Different authors have applied the compensation theory to assess moisture sorption processes of prickly pear seeds (Hassini et al., 2015) and figs (Hssaini et al., 2020), observing that these processes were also controlled by enthalpy.

## 4. Conclusion

The desorption processes of fresh jambolan pulp (JP) and jambolan seed (JS) were studied, and the latter one for the first time. JP isotherms were classified as type II - more to the solution-like, while JS isotherms followed the behavior of type II - more to the Langmuir-like, in the temperature range used (25–55 °C). The equilibrium moisture content (EMC) of both JP and JS were influenced by temperature, but JP is a product much more hygroscopic than JS. According to the monolayer moisture content ($m_o$), to avoid an unnecessary energy consumption in the drying process, the moisture content should not reach values below 7.8 g $H_2O$/100 g db for JP and 5.1 g $H_2O$/100 g db for JS. GAB and Oswin equations described with the best accuracy the desorption isotherms of JP and JS, respectively. The energies involved in the desorption process are higher for JP than JS, indicating that it is easier to dry JS. Still, the compensation theory has proven that the desorption phenomena for both pulp and seed of jambolan are enthalpy-driven mechanisms.

## Declarations

### *Author contribution statement*

Adriano Lucena de ARAÚJO: Performed the experiments; Analyzed and interpreted the data; Contributed reagents, materials, analysis tools or data; Wrote the paper.

Rosinelson da Silva PENA: Conceived and designed the experiments; Analyzed and interpreted the data; Contributed reagents, materials, analysis tools or data; Wrote the paper.

### *Funding statement*

This work was supported by the Conselho Nacional de Desenvolvimento Científico e Tecnológico (CNPq, Brazil) (422739/2016-2), and PROPESP (UFPA, Brazil). A. L. Araújo was supported by Coordenação de Aperfeiçoamento de Pessoal de Nível Superior (CAPES, Brazil) for their scholarship (01602743207).

### *Data availability statement*

Data included in article/supplementary material/referenced in article.

### *Declaration of interests statement*

The authors declare no conflict of interest.

### *Additional information*

No additional information is available for this paper.

## References


Aguilera, J.M., Stanley, D.W., 1999. Microstructural Principles of Food Processing and Engineering. Springer.

Ah-hen, K.S., Lemus-mondaca, R., Mathias-rettig, K.A., Vega-gálvez, A., López, J., 2014. Moisture sorption isotherms, isosteric heat of sorption and glass transition temperature of murtilla (*Ugni molinae* T.) berry. Int. J. Food Eng. 10 (4), 583–594.

Alpizar-reyes, E., Carrillo-navas, H., Romero-romero, R., Varela Guerrero, V., Alvarez-ramírez, J., Pérez-alonso, C., 2017. Thermodynamic sorption properties and glass transition temperature of tamarind seed mucilage (*Tamarindus indica* L.). Food Bioprod. Process. 101, 166–176.

AOAC - Association of Official Analytical Chemists, 2010. Official Methods of Analysis of the AOAC International, eighteenth ed. Arlington.

Aqil, F., Munagala, R., Jeybalan, J., Joshi, T., Gupta, R.C., Singh, I.P., 2014. The Indian blackberry (Jamun), antioxidant capacity, and cancer protection. In: Preddy, V.R. (Ed.), Cancer: Oxidative Stress and Dietary Antioxidants. Academic Press, pp. 101–113.

Araújo, A.L., Pena, R.S., 2020. Effect of particle size and temperature on the hygroscopic behaviour of cassava flour from dry group and storage time estimation. CyTA - J. Food 18 (1), 178–186.

Araújo, A.L., Pena, R.S., 2021. Influence of process conditions on the mass transfer of osmotically dehydrated jambolan fruits. Food Sci. Technol. ahead of print.

Aslan-tontul, S., 2020. Moisture sorption isotherm and thermodynamic analysis of quinoa grains. Heat Mass Tran. 57, 543–550.

Biswall, S., Mohapatra, M., Panda, M.K., Dash, S.K., 2017. Moisture desorption isotherms of fresh Jamun (*Syzygium cumini*) fruit. Indian J. Agric. Res. 51 (3), 267–271.

Bowman, A.W., Robinson, D.R., 1990. Introduction to Regression and Analysis of Variance. IOP Publishing.

Brunauer, S., Emmet, P.H., Teller, E., 1938. Adsorption of gases in multimolecular layers. J. Am. Chem. Soc. 60 (2), 309–319.

Chirife, J., Iglesias, H.A., 1978. Equations for fitting water sorption isotherms of foods. Part 1 – a review. J. Food Technol. 13, 159–174.

Chowdhury, T., Das, M., 2010. Moisture sorption isotherm and isosteric heat of sorption characteristics of starch based edible films containing antimicrobial preservative. Int. Food Res. J. 17 (3), 601–614.

Damodaran, S., 2017. Water and ice relations in foods. In: Damodaran, S., Parkin, K.L. (Eds.), Fennema's Food Chemistry. CRC Press, pp. 19–91.

Eim, V.S., Roselló, C., Femenia, A., Simal, S., 2011. Moisture sorption isotherms and thermodynamic properties of carrot. Int. J. Food Eng. 7 (3), 1–18.

Falade, K., Aworh, O., 2004. Adsorption isotherms of osmo-oven dried African star apple (*Chrysophyllum albidum*) and African mango (*Irvingia gabonensis*) slices. Eur. Food Res. Technol. 218, 278–283.

FAO - Food and Agriculture Organization of the United Nations, 2003. Food Energy – Methods of Analysis and Conversion Factors, 77th ed. Rome.

Faria, A.F., Marques, M.C., Mercadante, A.Z., 2011. Idenfication of bioactive compounds from jambolão (*Syzygium cumini*) and antioxidant capacity evaluation in different pH conditions. Food Chem. 126 (15), 1571–1578.

Hassini, L., Bettaieb, E., Desmorieux, H., Torres, S.S., Touil, A., 2015. Desorption isotherms and thermodynamic properties of prickly pear seeds. Ind. Crop. Prod. 67, 457–465.

Hercigonja, R., Rakic, V., 2015. Enthalpy-entropy compensation for n-hexane adsorption on Y zeolite containing transition metal cations. Sci. Sinter. 47 (1), 83.

Hssaini, L., Ouabou, R., Charafi, J., Idliman, A., Lamharrar, A., Razouk, R., Hanine, H., 2020. Hygroscopic proprieties of fig (*Ficus carica* L.): mathematical modelling of moisture sorption isotherms and isosteric heat kinetics. South Afr. J. Bot.

INMET – Instituto Nacional de Meteorologia, 1992. Normas Climatológicas. Retrieved from. http://www.inmet.gov.br/portal/index.php?R=bdmep/bdmep.

Khiari, R., Zemni, H., Maury, C., Mihoubi, D., 2020. Modeling desorption isotherms and thermodynamic properties of Italia grapes. J. Food Process. Preserv. 44 (10), 1–13.

Krug, R.R., Hunter, W.G., Grieger, R.A., 1976. Enthalpy-entropy compensation: some fundamental statistical problems associated with analysis of Van't Hoff and Arrhenius data. J. Phys. Chem. 80, 2335–2341.

Maroulis, Z.B., Tsami, E., Arinos-kouris, D., Saravacos, G.D., 1988. Application of the GAB model to the sorption isotherms for dried fruits. J. Food Eng. 7, 63–70.

Mulet, A., García-reverter, J., Sanjuan, R., Bon, J., 1999. Sorption isosteric heat determination by thermal analysis and sorption isotherms. J. Food Sci. 64, 64–68.

Nascimento, A., Cavalcanti-mata, M.E., Martins Duarte, M.E., Pasquali, M., Lisboa, H.M., 2019. Construction of a design space for goat milk powder production using moisture sorption isotherms. J. Food Process. Eng. 42 (6), 1–11.

Oliveira, D.E.C., Resende, O., Costa, L.M., Silva, H.W., 2017. Thermodynamic properties of crambe fruits. Acta Sci. Agron. 39 (3), 291–298.

Oulahna, D., Hebrard, A., Cuq, B., Abecassis, J., Fages, J., 2012. Agglomeration of durum wheat semolina: thermodynamic approaches for hydration properties measurements. J. Food Eng. 109 (3), 619–626.

Pahlevanzadeh, H., Yazdani, M., 2005. Moisture adsorption isotherms and isosteric energy for almond. J. Food Process. Eng. 28 (4), 331–345.

Palipane, K.B., Driscoll, R.H., 1993. Moisture sorption characteristics of in-shell macadamia nuts. J. Food Eng. 18 (1), 63–76.

Paul, I.D., Das, M., 2019. Moisture sorption isotherm and thermodynamic properties of jamun (*Syzygium cumini* L.) powder made from jamun pulp and seed. Int. J. Food Stu. 8, 111–126.

Peng, G., Chen, X., Wu, W., Jiang, X., 2007. Modeling of water sorption isotherm for corn starch. J. Food Eng. 80 (2), 562–567.

Prette, A.P., Almeida, F.A.C., Villa-véllez, H.A., Telis-romero, J., 2013. Thermodynamic properties of water sorption of jackfruit (*Artocarpus heterophyllus* Lam.) as a function of moisture content. Food Sci. Technol. 33 (1), 199–208.

Rahman, M.S., 2009. Food stability beyond water activity and glass transition: macro-micro region concept in the state diagram. Int. J. Food Prop. 12 (4), 726–740.

Rizvi, S.S.H., 2014. Thermodynamic properties of foods in dehydration. In: Rao, M.A., Rizvi, S.S.H., Datta, A.K., Ahmed, J. (Eds.), Engineering Properties of Foods. CRC Press, pp. 359–436.

Sabino, L.B.S., Brito, E.S., Silva-Júnior, I.J., 2018. Jambolan – Syzygium jambolanun. In: Rodrigues, S., Silva, E.O., Brito, E.S. (Eds.), Exotic Frutis. Academic Press, pp. 251–256.

Santana, R.F., Oliveira Neto, E.R., Santos, A.V., Soares, C.M.F., Lima, A.S., Cardoso, J.C., 2014. Water sorption isotherm and glass transition temperature of freeze-dried *Syzygium cumini* fruit (Jambolan). J. Therm. Anal. Calorim. 120 (1), 519–524.

Scott, W.J., 1957. Water relations of food spoilage microorganisms. Adv. Food Res. 7, 83–127.

Sormoli, M.E., Langrish, T.A.G., 2015. Moisture sorption isotherms and net isosteric heat of sorption for spray-dried pure orange juice powder. LWT - Food Sci. Technol. (Lebensmittel-Wissenschaft -Technol.) 62, 875–882.

Yanniotis, S., Blahovec, J., 2009. Model analysis of sorption isotherms. LWT - Food Sci. Technol. (Lebensmittel-Wissenschaft -Technol.) 42, 1688–1695.

Zeymer, J.S., Corrêa, P.C., Oliveira, G.H.H., Baptestini, F.M., Faria, I.L., 2018. Thermodynamic properties of sorption of rice in the husk. Eng. Agrícola 38 (3), 369–375.

Zeymer, J.S., Corrêa, P.C., Oliveira, G.H.H., Araújo, M.E.V., Magalhães, D.S., 2020. Thermodynamic properties of moisture desorption isotherms of ryegrass (*Lolium multiflorum* L.) seeds. Cienc. E Agrotecnol 44.